J Membrane Biol (2012) 245:51–68
DOI 10.1007/s00232-011-9412-4

REVIEW

Functions of Cholesterol and the Cholesterol Bilayer Domain Specific to the Fiber-Cell Plasma Membrane of the Eye Lens

Witold K. Subczynski · Marija Raguz · Justyna Widomska · Laxman Mainali · Alexey Konovalov

Received: 30 August 2011 / Accepted: 29 November 2011 / Published online: 30 December 2011

Abstract The most unique feature of the eye lens fiber-cell plasma membrane is its extremely high cholesterol content. Cholesterol saturates the bulk phospholipid bilayer and induces formation of immiscible cholesterol bilayer domains (CBDs) within the membrane. Our results (based on EPR spin-labeling experiments with lens-lipid membranes), along with a literature search, have allowed us to identify the significant functions of cholesterol specific to the fiber-cell plasma membrane, which are manifest through cholesterol–membrane interactions. The crucial role is played by the CBD. The presence of the CBD ensures that the surrounding phospholipid bilayer is saturated with cholesterol. The saturating cholesterol content in fiber-cell membranes keeps the bulk physical properties of lens-lipid membranes consistent and independent of changes in phospholipid composition. Thus, the CBD helps to maintain lens-membrane homeostasis when the membrane phospholipid composition changes significantly. The CBD raises the barrier for oxygen transport across the fiber-cell membrane, which should help to maintain a low oxygen concentration in the lens interior. It is hypothesized that the appearance of the CBD in the fiber-cell membrane is controlled by the phospholipid composition of the membrane. Saturation with cholesterol smoothes the phospholipid-bilayer surface, which should decrease light scattering and help to maintain lens transparency. Other functions of cholesterol include formation of hydrophobic and rigidity barriers across the bulk phospholipid-cholesterol domain and formation of hydrophobic channels in the central region of the membrane for transport of small, nonpolar molecules parallel to the membrane surface. In this review, we provide data supporting these hypotheses.

Keywords Lens lipid · Lens cortex · Lens nucleus · Cholesterol bilayer domain · Spin label · Electron paramagnetic resonance

W. K. Subczynski (✉) · M. Raguz · J. Widomska · L. Mainali · A. Konovalov
Department of Biophysics, Medical College of Wisconsin, 8701 Watertown Plank Road, Milwaukee, WI 53226, USA
e-mail: subczyn@mcw.edu

M. Raguz
Department of Medical Physics and Biophysics, School of Medicine, University of Split, Split, Croatia

J. Widomska
Department of Biophysics, Medical University, Lublin, Poland

Introduction

The eye lens is an avascular structure which, in conjunction with the cornea, focuses light on the retina and, thus, must remain transparent throughout an individual's life. The human lens is 9 mm in diameter and 4 mm thick and contains 1,000–3,000 layers of fiber cells (Fig. 1). To prevent excessive light scattering and compromised lens transparency, fiber cells lose all of their subcellular organelles during maturation (Beebe 2003). Newly formed fiber cells in the periphery displace existing fiber cells near the center of the lens (Beebe 2003). Thus, the line from the lens surface to its center is the age axis. Fiber cells are not homogeneous in terms of composition, metabolism or age. The adult lens contains two kinds of fiber cells: those located in the cortex (the outer layers of the lens), which are not yet mature and still contain organelles (including mitochondria), and those located in the nucleus (the core of the lens), which are mature and do not contain organelles (Fig. 1). The nuclear region contains the embryonic lens,

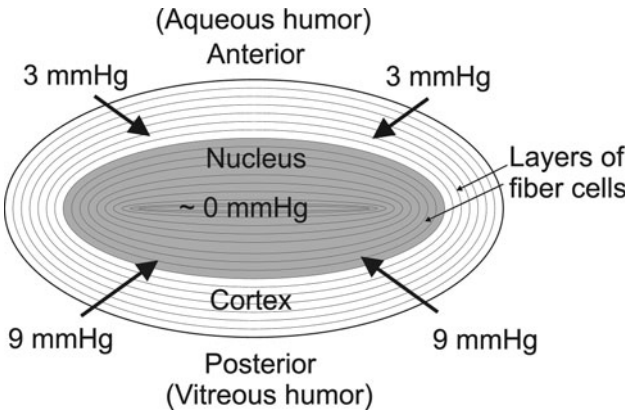

Fig. 1 Diagram of the eye lens section showing the location of the lens cortex and nucleus. Values of the oxygen partial pressure at the surface of the anterior and posterior cortex of the lens in the healthy eye are taken from Siegfried et al. (2010). *Arrows* indicate the oxygen flux into the lens, toward the lens center. The Chol/PL mole ratio in cortical fiber-cell membranes is from 1 to 2 and that in nuclear membranes is from 3 to 4 (Li et al. 1987). The basic phospholipid composition (taken from Yappert et al. 2003 for a 25 year old human) of the cortical and nuclear lens lipid membrane is 3.2% PC, 14% PE, 1.5% PS and 42.8% (DHSM + SM) and 0.7% PC, 6% PE, 3.1% PS and 49.8% (DHSM + SM), respectively. PC, phosphatidylcholine; PE, phosphatidylethanolamine; PS, phosphatidylserine; SM, sphingomyelin (including dihydrosphingomyelin)

the fetal fibers and the juvenile and adult nuclear fibers (Li et al. 1985). Due to minimal cell turnover, cells in the nucleus of the human lens are considered the longest-living cells in the human body (Peterson and Delamere 1992). Consequently, they require functional mechanisms to protect them from damage.

Membranes of fiber cells, which build the human eye lens (Fig. 1), are overloaded with cholesterol, which not only saturates the phospholipid bilayer but also leads to the formation of cholesterol bilayer domains (CBDs) within these membranes (Jacob et al. 1999, 2001). The appearance of these domains is usually a sign of pathology (Tulenko et al. 1998). However, only in the eye lens can CBDs play a positive physiological function, maintaining lens transparency (Borchman et al. 1996; Jacob et al. 1999; Mason et al. 2003) and, therefore, possibly protecting against cataract formation (Jacob et al. 1999; Mason et al. 2003). The significance of cholesterol in the eye lens is further emphasized by observations that inherited defects in enzymes of cholesterol metabolism and the use of cholesterol biosynthesis–inhibiting drugs cause cataract formation in humans and other animals (Borchman et al. 1989; Cenedella 1996; de Vries and Cohen 1993; Kirby 1967; Mosley et al. 1989). These effects indicate that cholesterol plays an important physiological role in the eye lens. A better understanding of the physiological functions of cholesterol requires an increased understanding of cholesterol function at the molecular level, which can be shown through cholesterol-induced changes in the properties of the lipid-bilayer portion of the fiber-cell plasma membrane. Changes in cholesterol content in the fiber-cell plasma membrane, which occur during aging, are indicated by an increase in the total cholesterol/phospholipid (Chol/PL) molar ratio and as a higher Chol/PL molar ratio in the nucleus compared to the cortex (Borchman et al. 1989; Fleschner and Cenedella 1991; Li and So 1987; Raguz et al. 2009; Rujoi et al. 2003). Interestingly, animals with a long life span exhibit a higher Chol/PL molar ratio than animals with a shorter life span (Borchman et al. 1989; Fleschner and Cenedella 1991; Li et al. 1987). Also, the phospholipid composition of the eye-lens membrane changes significantly with age (Huang et al. 2005; Paterson et al. 1997; Truscott 2000; Yappert et al. 2003), between regions of the lens (Raguz et al. 2009, 2004) and between animal species (Borchman et al. 2004; Deeley et al. 2008). In contrast, there is not much difference in the lipid composition of most organs from one species to another (Rouser et al. 1969, 1971) or with age (Rouser and Solomon 1969). Such great variation with age in phospholipid composition and cholesterol content suggests difficulties in maintaining fiber-cell-membrane homeostasis as well as homeostasis within the fiber cell, which is required for lens transparency. This is especially true for fiber cells in which the plasma membrane is basically the only membranous structure. Lens fiber cells lose their intracellular organelles soon after they are formed (Rafferty 1985), and the plasma membrane accounts for essentially all lens lipids.

The need for a high cholesterol content in the lens is unclear. Borchman et al. (2004), based on their measurements and data from the literature, hypothesized that lens membranes are highly ordered because of high sphingolipid and cholesterol contents and suggested that cholesterol provides buffering properties for membrane fluidity by ordering fluid phospholipids and disordering ordered lipids (Li et al. 1987; Truscott 2000). They concluded that the physiological role of cholesterol is to increase the structural order of cortical membrane lipids and decrease the order of nuclear lipids so that the two membranes have a similar order (Borchman et al. 1996). Because cholesterol is relatively stable and resistant to oxidation compared with unsaturated phospholipids, it is suggested that it may also add chemical stability to the membrane (Borchman and Yappert 2010). Additionally, the high cholesterol level may be related to gap junctions. Cholesterol is understood to be associated with gap junctions (Biswas et al. 2009, 2010; Biswas and Lo 2007), and the lens contains more gap junctions than any other tissue. Cholesterol content in protrusions, which are specialized, interlocking membrane domains between lens fiber cells, is very high. It has been suggested (Biswas et al. 2010) that the high cholesterol content in protrusion membranes makes them less

deformable and more suitable to maintain fiber-to-fiber stability during visual accommodation. The relationship between lens cholesterol and lens cataracts has been reviewed (Cenedella 1996) with an ultimate focus on the effect of statin drugs on the lens in humans and other animals.

We present data that support the main hypothesis of this review: a high cholesterol content and the presence of the CBD are necessary to maintain lens-membrane homeostasis throughout the life of an individual. It should be stressed here that, due to minimal cell turnover, cells in the lens nucleus may be the longest-lived cells in the human body (Peterson and Delamere 1992). Please note that hypotheses presented in this review regarding the purported functions of cholesterol and CBDs are based on measurements for lens-lipid membranes and model lipid membranes—i.e., membranes without a protein component. In these measurements, we have mostly used electron paramagnetic resonance (EPR) spin-labeling methods. The unique abilities of these methods will first be described, to provide guidelines for a clear understanding of our experimental results and our interpretation of data.

EPR Spin-Labeling Approaches for Profiles of Lens-Lipid Membrane Properties

EPR spin-labeling methods provide a unique opportunity to determine the lateral organization of lipid bilayer membranes, including coexisting membrane domains or coexisting membrane phases (Ashikawa et al. 1994; Kawasaki et al. 2001; Raguz et al. 2008; Subczynski et al. 2007a, 2007b). These methods also provide a number of approaches to determine several important membrane properties as a function of bilayer depth, including alkyl-chain order (Marsh 1981), fluidity (Subczynski et al. 2010), hydrophobicity (Subczynski et al. 1994) and the oxygen diffusion-concentration product (called the "oxygen transport parameter") (Kusumi et al. 1982). In some cases, these properties can be obtained in coexisting membrane domains without the need for their physical separation (Subczynski et al. 2007a, 2010). We will briefly explain how EPR spin-labeling methods can be used to obtain profiles of the above-mentioned properties across lens-lipid membranes and simple model membranes, which resemble the basic lipid composition of lens membranes (Mainali et al. 2011b; Raguz et al. 2008, 2009; Widomska et al. 2007a).

In these studies, phospholipid- and cholesterol-analogue spin labels are incorporated in the membrane with the nitroxide moiety, which gives rise to the observed EPR signal, at specific depths and in specific membrane domains. The physical/chemical properties of the microenvironment in the immediate vicinity of the nitroxide are then characterized using EPR spectroscopic methods. The spin labels used here have molecular structures similar to phospholipids or cholesterol and, therefore, should approximate cholesterol–phospholipid and cholesterol–cholesterol interactions in the membrane as well as be distributed between different membrane domains similarly to parent molecules (Raguz et al. 2008, 2009; Widomska et al. 2007a). Figure 2 is a schematic drawing that shows possible cases of spin-label distribution that may be relevant to eye-lens-lipid membranes.

When the cholesterol concentration in the membrane is close to its solubility threshold, the entire membrane should be in the liquid-ordered-like phase. In this case, separate domains are not expected (Fig. 2a). Profiles of the order parameter, fluidity, hydrophobicity and the oxygen transport parameter can be obtained in this homogeneous membrane. In the case of membranes oversaturated with

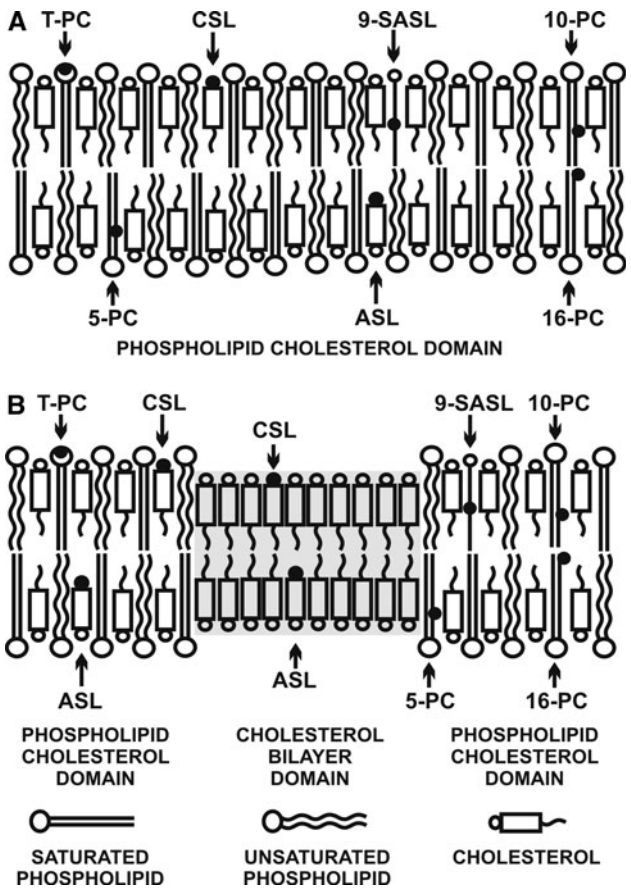

Fig. 2 Schematic drawings showing organization of lipids and spin-label distributions that may be relevant to eye-lens lipid membranes. The distribution and approximate localization of the nitroxide moiety of lipid spin labels (phospholipid analogues 5-, 10-, 16- T-PC and 9-SASL and cholesterol analogues ASL and CSL) in membranes with a cholesterol content close to the CST (**a**, model of the lens lipid membrane from young animals and the cortical membrane) and in membranes oversaturated with cholesterol, when the bulk PCD coexists with the CBD (**b**, model of the nuclear membrane). The nitroxide moieties of spin labels are indicated by *black dots*

cholesterol, in which CBDs are formed, the distribution of lipid spin labels is unique (Fig. 2b). The phospholipid-analogue spin labels should partition only into the bulk phospholipid cholesterol domain (PCD, the phospholipid cholesterol membrane saturated with cholesterol before formation of the CBD or the phospholipid cholesterol membrane coexisting with the CBD), and the cholesterol analogues should distribute between the two domains. Thus, only cholesterol-analogue spin labels can discriminate the two coexisting domains. The unique distribution of phospholipid-analogue spin labels allows profiles of the order parameter, fluidity, hydrophobicity and oxygen transport parameter to be obtained in the bulk PCD without "contamination" from the CBD. These two cases are relevant to lens-lipid membranes that are near the cholesterol solubility threshold (CST) in the lenses of young animals and in the cortex of lenses from older animals and humans (Fig. 2a) and are oversaturated with cholesterol (the coexisting CBD and PCD are present) in the lens nucleus (Fig. 2b).

The CBD Saturates the Surrounding Phospholipid Bilayer with Cholesterol

The lipid composition of the lens fiber-cell membrane changes as both humans and other animals age (Borchman et al. 1994; Broekhuyse 1973; Broekhuyse and Kuhlmann 1974, 1978; Huang et al. 2005; Li and So 1987; Li et al. 1985, 1987; Roy et al. 1982; Rujoi et al. 2003; Truscott 2000; Yappert et al. 2003). Usually, such notable changes would result in alteration of the physical properties of the membrane, which would then affect the function of proteins immersed in the lipid bilayer (Epand 2005). Based on results obtained for lens-lipid membranes from different species (a 6 month old calf and pig [Raguz et al. 2008; Widomska et al. 2007a]), from animals at different ages (6 month old and 2 year old cow and pig [Mainali et al. 2011b; Raguz et al. 2009; Widomska et al. 2007a]) and from different eye regions (the cortex and nucleus of a 2 year old cow and pig [Mainali et al. 2011b; Raguz et al. 2009]), we conclude that the extremely high (saturating) content of cholesterol in the fiber-cell membrane keeps the bulk physical properties of the lipid-bilayer portion of the membrane consistent and independent of changes in the phospholipid composition. The phospholipid composition of fiber-cell membranes significantly changes not only between species (Deeley et al. 2008; Yappert and Borchman 2004; Yappert et al. 2003) and with age (Yappert and Borchman 2004) but also between different regions of the lens (Li and So 1987; Li et al. 1987; Raguz et al. 2009). Surprisingly, independent of these differences, profiles of the bulk membrane properties across PCDs were very similar (practically identical) in all of the investigated membranes. Bulk membrane properties included the order parameter, fluidity, hydrophobicity and the oxygen transport parameter (oxygen diffusion-concentration product). As we stated in the Introduction, a similar conclusion was made by Borchman et al. (1996) using the structural order parameter as a measure of fluidity in bovine cortical and nuclear lens-lipid membranes. They showed that at a saturating amount of cholesterol the structural orders of nuclear and cortical membranes are very similar and concluded that the physiological role of cholesterol is to increase the structural order of cortical membrane lipids and to decrease the order of nuclear lipids so that the two membranes have a similar order. This finding agrees with our main conclusion.

To illustrate this conclusion, profiles of the order parameter (Fig. 3a–d), fluidity (Fig. 3e–h), hydrophobicity (Fig. 4a–d) and the oxygen transport parameter (Fig. 4e–h) across the PCD of the lens-lipid membrane from a 6 month old pig and calf (Figs. 3a, e and 4a, e) and from the cortex and nucleus of a 2 year-old pig (Figs. 3c, g and 4c, g) and cow (Figs. 3d, h and 4d, h) are presented. With this method, we can compare the differences between species as well as age-related and/or topographical differences, if any, in the bulk properties of the lens-lipid membrane. All profiles were obtained with phospholipid-type spin labels, which describe properties of the PCD. We should reiterate that in all investigated membranes the cholesterol content was close to or in excess of the CST. Small differences in the hydrophobicity profiles shown in Fig. 4a, d suggest that 6 month old pig and 2 year old cow cortex membranes are not yet saturated with cholesterol (Raguz et al. 2008, 2009).

All profiles for membranes with a saturating amount of cholesterol differ drastically from profiles across membranes without cholesterol. This is illustrated in Figs. 5a, d

Fig. 3 Independently of the differences in the phospholipid composition of lens-lipid membranes derived from the eyes of different species, different animal ages and different region of the lens, the profiles of the membrane order (the alkyl-chain order parameter) and the membrane dynamics (spin–lattice relaxation time) across these membranes are very similar. Profiles of the alkyl-chain order parameter (**a**–**d**) and the membrane fluidity (spin–lattice relaxation time, T_1, for deoxygenated samples) (**e**–**h**) obtained at 35°C across the PCD of lens-lipid membranes made of lipids extracted from a 6 month old pig and calf (**a**, **e**), a 6 month old pig after addition of excess cholesterol (**b**, **f**) and the cortex and nucleus of a 2 year old pig (**c**, **g**) and cow (**d**, **h**). Approximate localizations of the nitroxide moieties of spin labels are indicated by *arrows*. The order parameter is a measure of the amplitude of the wobbling motion of the alkyl-chain fragment to which the nitroxide moiety is attached (Hubbel and McConnell 1968), while T_1 depends primarily on the rate of motion of the nitroxide moiety within the lipid bilayer and, thus, describes the dynamics of the membrane environment at a depth at which the nitroxide fragment is located (Mainali et al. 2011a). Data compiled from Raguz et al. (2008, 2009) and Widomska et al. (2007a)

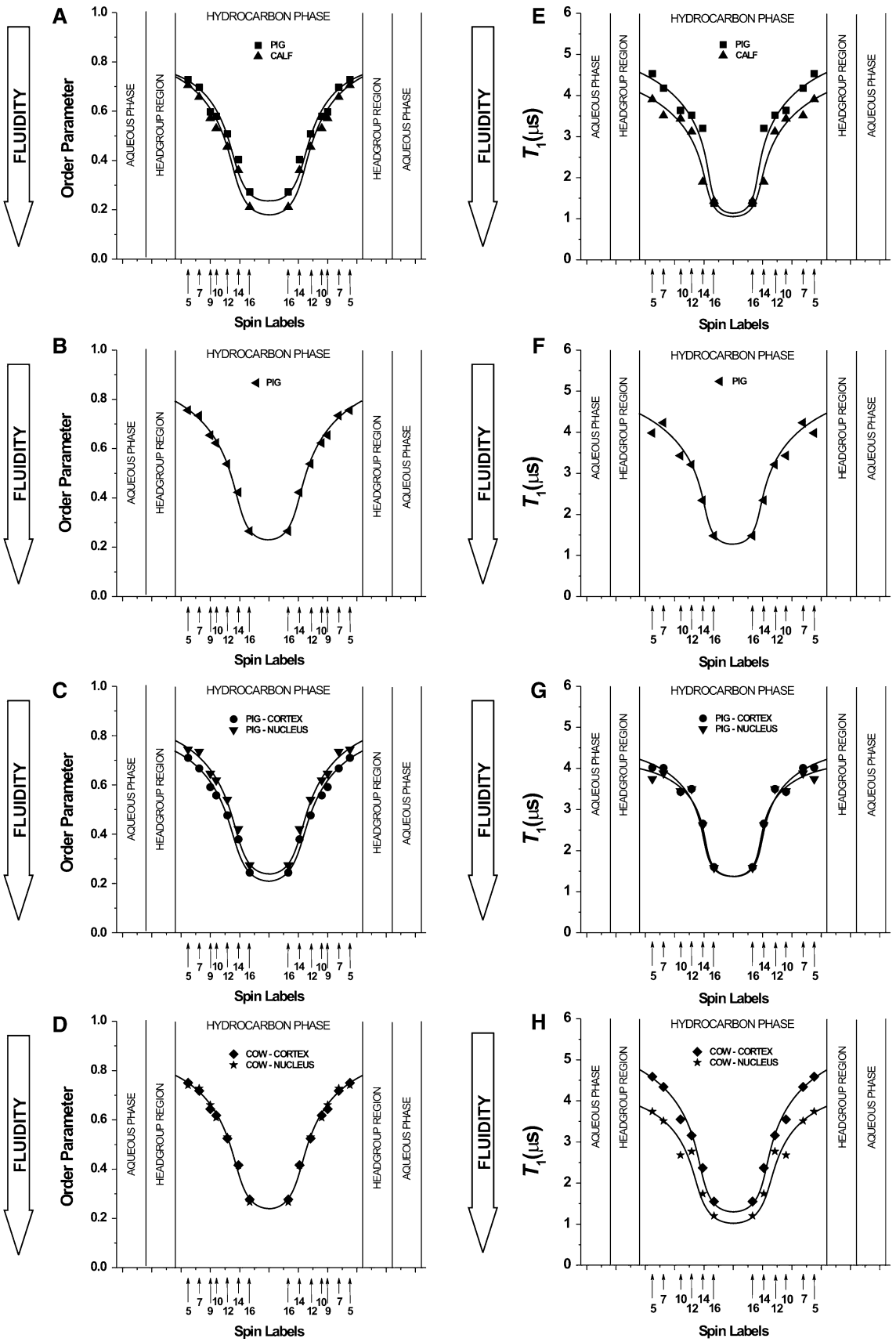
A
B
C
D
E
F
G
H
FLUIDITY
Order Parameter
T_1(μs)
AQUEOUS PHASE
HEADGROUP REGION
HYDROCARBON PHASE
HEADGROUP REGION
AQUEOUS PHASE
PIG
CALF
PIG - CORTEX
PIG - NUCLEUS
COW - CORTEX
COW - NUCLEUS
5 7 9 10 12 14 16 16 14 12 10 9 7 5
Spin Labels

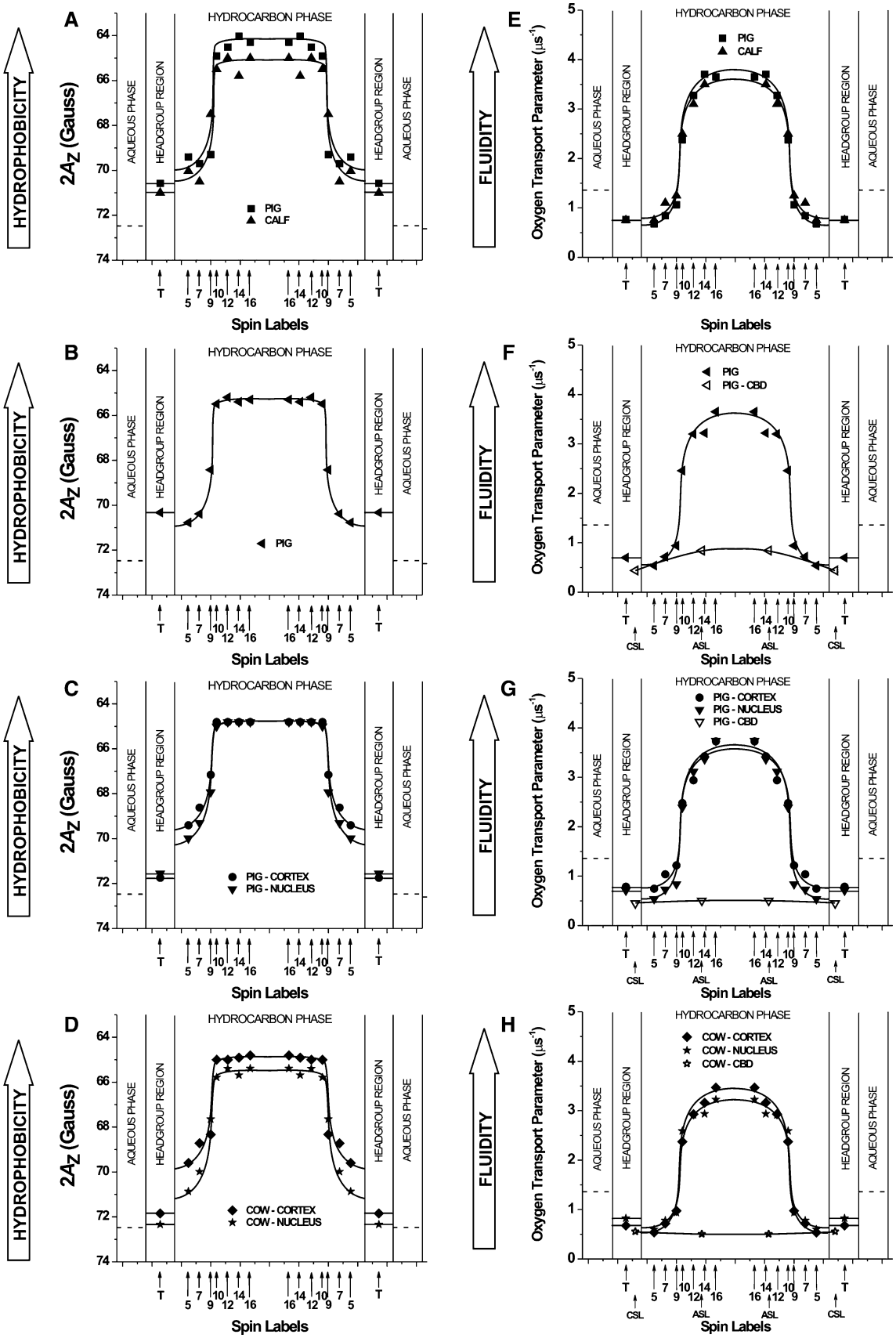
A
B
C
D
E
F
G
H
HYDROCARBON PHASE
AQUEOUS PHASE
HEADGROUP REGION
HYDROPHOBICITY
FLUIDITY
2Az (Gauss)
Oxygen Transport Parameter (μs-1)
Spin Labels
PIG
CALF
PIG - CBD
PIG - CORTEX
PIG - NUCLEUS
COW - CORTEX
COW - NUCLEUS
COW - CBD
T
CSL
ASL

◀ **Fig. 4** Independently of the differences in the phospholipid composition of lens-lipid membranes, all these membranes have a very similar shape of the hydrophobic barrier, with hydrophobicity in the membrane center close to that of hexane ($\varepsilon = 2$). Also, profiles of the oxygen transport parameters are nearly identical with low oxygen transport close to the membrane surface and high oxygen transport in the membrane center. Hydrophobicity profiles (obtained at −165°C) (**a**–**d**) and profiles of the oxygen transport parameter (obtained at 35°C) (**e**–**h**) across the PCD of lens-lipid membranes made of lipids extracted from a 6 month old pig and calf (**a**, **e**), a 6 month old pig after addition of cholesterol (**b**, **f**), and the cortex and nucleus of a 2 year old pig (**c**, **g**) and cow (**d**, **h**). Profiles of the oxygen transport parameter across the CBD, which is formed in lens-lipid membranes made of lipids extracted from a 6 month old pig after addition of cholesterol (**f**) and from the nucleus of a 2 year old pig (**g**) and a 2 year old cow (**h**), are also included. *Broken lines* indicate the appropriate value in the aqueous phase. Approximate localizations of nitroxide moieties of spin labels are indicated by *arrows*. Hydrophobicity profiles ($2A_Z$) are obtained for frozen samples to eliminate the motional contribution. Smaller $2A_Z$ values (upward changes in the profiles) indicate higher hydrophobicity. Usually, the local hydrophobicity as observed by $2A_Z$ is related to the hydrophobicity (or ε) of the bulk organic solvent by referring to Fig. 2 in Subczynski et al. (1994). An oxygen transport parameter was introduced as a convenient quantitative measure of the collision rate between the spin label and molecular oxygen (Kusumi et al. 1982). It is useful to monitor membrane fluidity, which reports on translational diffusion of small molecules. The oxygen transport parameter is normalized to an oxygen concentration that corresponds to the sample equilibrated with atmospheric air. Data compiled from Raguz et al. 2008, 2009) and Widomska et al. (2007a)

and 6a, d, where profiles for the POPC membrane and the POPC membrane saturated with cholesterol are shown; in Figs. 5b, e and 6b, e, which show profiles for the egg sphingomyelin (ESM) membrane and the ESM membrane saturated with cholesterol; and in Figs. 5c, f and 6c, f, which display profiles across the model membrane, made from a phospholipid mixture that resembles the composition of the pig lens-lipid membrane (Deeley et al. 2008), without cholesterol and saturated with cholesterol.

Profiles of the order parameter (Fig. 5a–c) indicated that in membranes saturated with cholesterol, including lens-lipid membranes (Fig. 3a–d), lipids are strongly ordered at all depths, which is in contrast to the low order of membranes without cholesterol (Fig. 5a–c). All profiles show a gradual decrease in alkyl-chain order with an increasing depth in the membrane. Values of the order parameter measured at the same depth are always significantly greater for membranes saturated with cholesterol than for membranes without cholesterol. Thus, an ordering effect of cholesterol in fluid-phase membranes is observed at all depths from the membrane surface to the membrane center. The order parameter, which is most often used as a measure of membrane fluidity, describes the amplitude of the wobbling motion of alkyl chains relative to the membrane normal and does not explicitly contain time or velocity (Hubbell and McConnell 1968). Thus, this parameter can be considered nondynamic.

The structural order determined by the static value of the *trans*/gauche rotamer ratio in the hydrocarbon chains (with special attention paid to the role of cholesterol) has been evaluated by other groups for lens-lipid membranes (Borchman et al. 1993, 1996, 1999). Thus, the structural order describes membrane properties averaged across membrane depths and domains, which is less informative than the profiles of the order parameter presented here. These profiles reflect the local order of hydrocarbon chains at different depths in the membrane.

The spin–lattice relaxation time (T_1) obtained from saturation-recovery EPR measurements of lipid spin labels in deoxygenated samples depends primarily on the rotational correlation time of the nitroxide moiety within the lipid bilayer. Thus, T_1 can be used as a convenient quantitative measure of membrane fluidity that reflects local membrane dynamics (Mainali et al. 2011a, b, c). T_1 profiles, which we call "profiles of membrane fluidity," obtained for membranes saturated with cholesterol (Fig. 5d–f), including lens-lipid membranes (Fig. 3e–h), are very similar. When compared with fluidity profiles without cholesterol (Fig. 5d–f), they reveal that cholesterol has a rigidifying effect only to the depth occupied by the rigid steroid-ring structure and a fluidizing effect at deeper locations. These effects cannot be differentiated by profiles of the order parameter.

Profiles of hydrophobicity (Fig. 6a–c) and the oxygen transport parameter (Fig. 6d–f) in membranes saturated with cholesterol and in lens-lipid membranes (Fig. 4a–h) have a characteristic rectangular shape with an abrupt change between the C9 and C10 positions, which is approximately where the rigid steroid-ring structure of cholesterol reaches into the membrane. At this position, hydrophobicity increases from the level of methanol to that of hexane and the oxygen transport parameter increases by a factor of ∼2.5 (from the level observed in gel-phase membranes to that observed in fluid-phase membranes). These profiles are bell-shaped in phospholipid membranes without cholesterol (Fig. 6a–f). These results indicate that a high, saturating cholesterol content is responsible for these unique profiles and unique properties of lens-lipid membranes. These profiles are also characteristic of liquid-ordered-phase membranes saturated with cholesterol (Mainali et al. 2011c, d; Subczynski et al. 1994, 2007b; Widomska et al. 2007a), which allows us to conclude that the entire PCD in the lens-lipid membrane is in the liquid-ordered-like phase.

The above conclusions were based on profiles obtained for lens-lipid membranes with Chol/PL molar ratios of ∼1, in which the CBD was not observed and lipids were organized as in Fig. 2a. Figures 3 and 4 contain profiles obtained for lens-lipid membranes with Chol/PL molar ratios of ∼2 (from the nucleus of 2 year old cow and pig

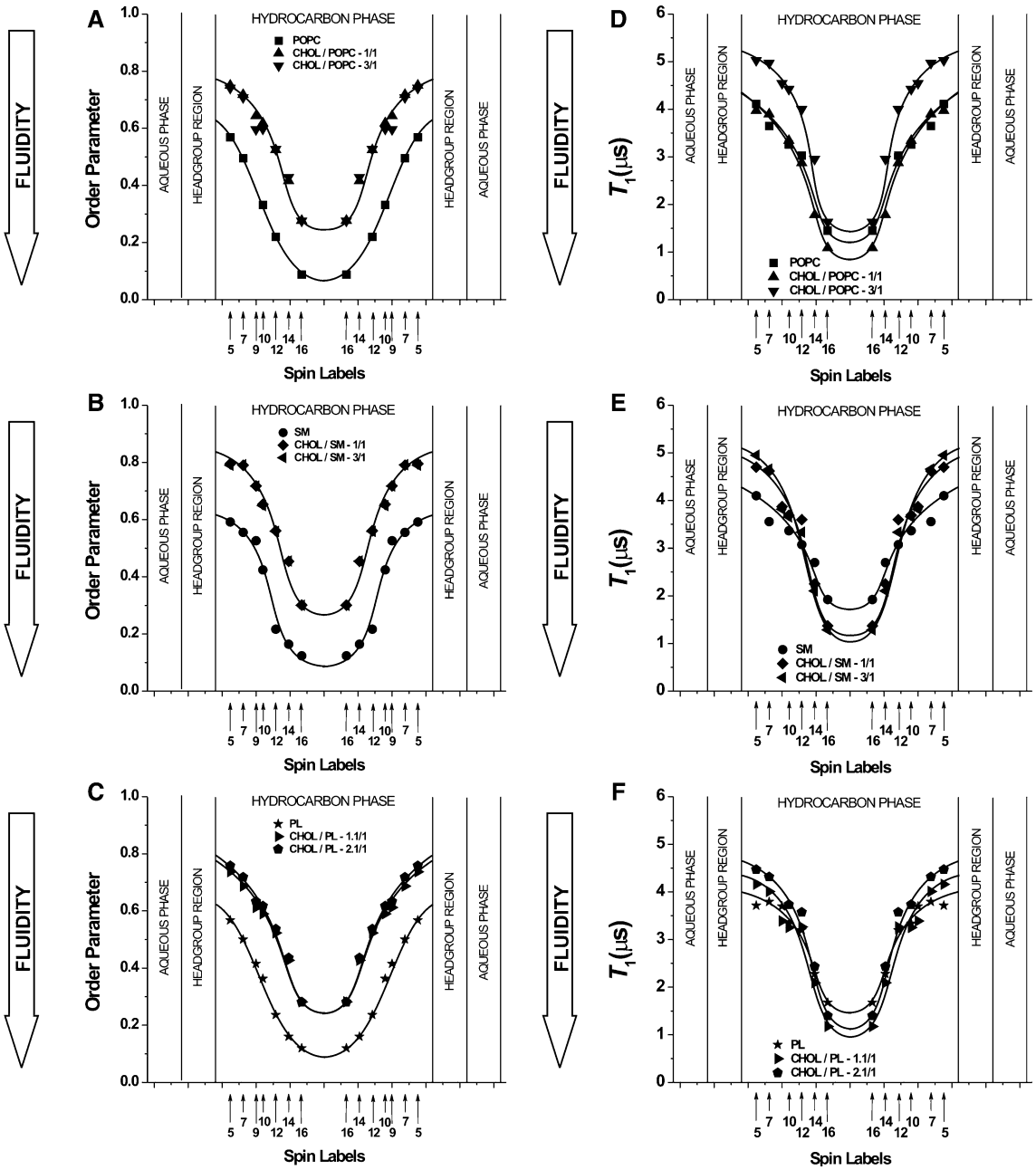

Fig. 5 An ordering effect of the saturating amount of cholesterol is observed at all depths from the membrane surface to the membrane center. However, profiles of membrane dynamics reveal that cholesterol has a rigidifying effect only to the depth occupied by the rigid steroid-ring structure and a fluidizing effect at deeper locations. Profiles of the alkyl-chain order parameter (**a**–**c**) and membrane fluidity (spin–lattice relaxation time, T_1, for deoxygenated samples) (**d**–**f**) obtained at 35°C across POPC membranes (**a**, **d**) without cholesterol (POPC) and with cholesterol at cholesterol/POPC mixing ratios of 1/1 (CHOL/POPC-1/1) and 3/1 (CHOL/POPC-3/1), across ESM membranes (**b**, **e**) without cholesterol (SM) and with cholesterol at cholesterol/SM mixing ratios of 2/1 (CHOL/SM-2/1) and 3/1 (CHOL/SM-3/1) and across model membranes made from a phospholipid mixture resembling the composition of the pig lens-lipid membrane (PL, 30% SM, 36% PC, 12% PE, 22% PS) (**c**, **f**) without cholesterol (PL), saturated with cholesterol at a cholesterol/PL mixing ratio of 1.1/1 (CHOL/PL-1.1/1) and oversaturated with cholesterol at a cholesterol/PL mixing ratio of 2.1/1 (CHOL/PL-2.1/1). Approximate localizations of nitroxide moieties of spin labels are indicated by *arrows*. Data compiled from Widomska et al. (2007a)

lens and from 6 month old pig lenses with the addition of excess cholesterol), in which the CBD was present and lipids were organized as in Fig. 2b. Profiles of the order parameter, fluidity, hydrophobicity and the oxygen transport parameter across the bulk PCD surrounding the CBD are very similar to those observed for membranes with a lower cholesterol content when the CBD is not yet observed. Similarly, profiles presented in Figs. 5 and 6 for

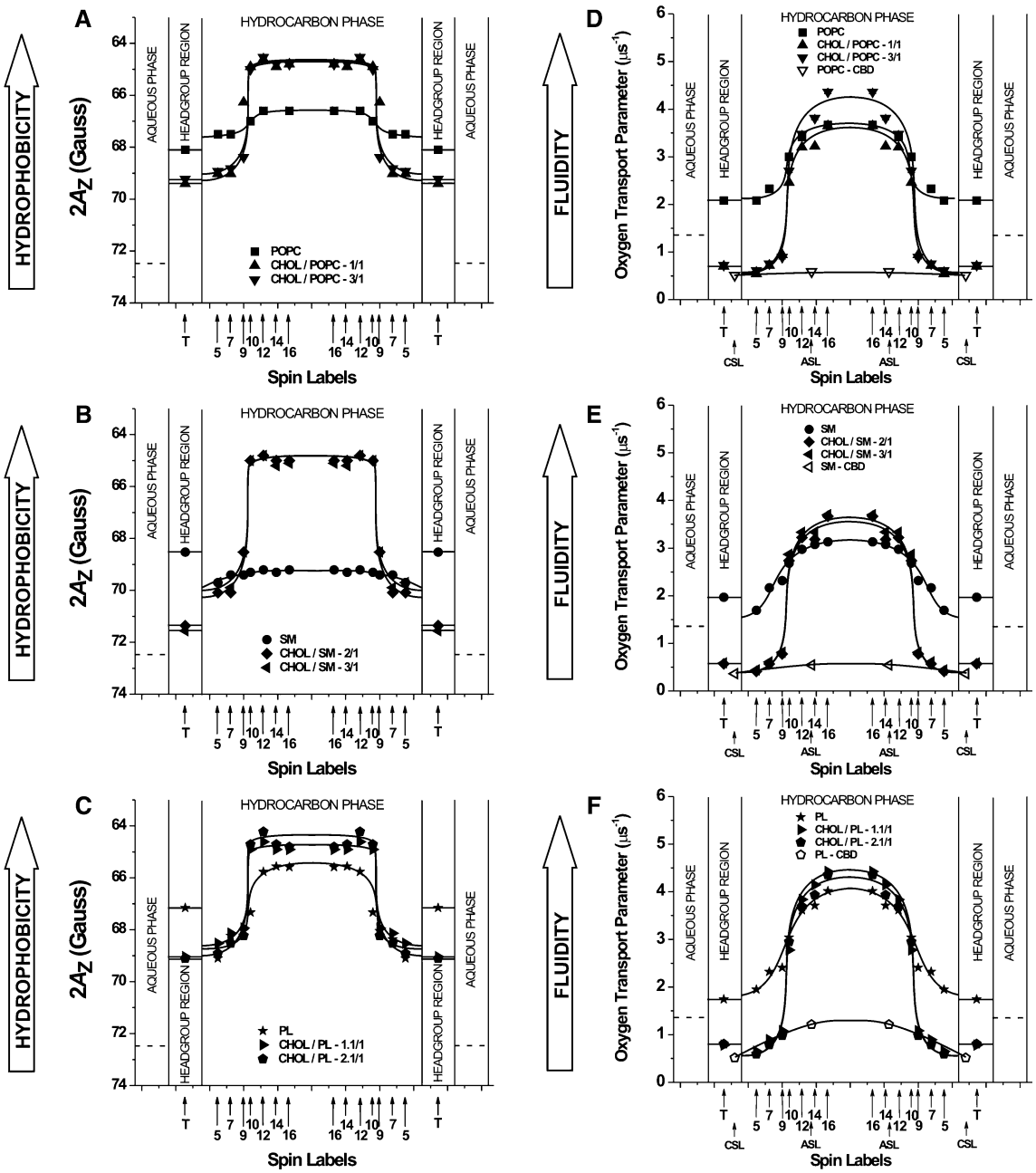

Fig. 6 The saturating amount of cholesterol is responsible for changing the bell-shaped hydrophobicity and oxygen transport parameter profiles to the rectangular shape with an abrupt change between C9 and C10 positions, which is approximately where the rigid steroid-ring structure of cholesterol reaches into the membrane. Hydrophobicity profiles (obtained at −165°C) (**a**–**c**) and profiles of the oxygen transport parameter (obtained at 35°C) (**d**–**f**) across POPC membranes (**a**, **d**), SM membranes (**b**, **e**) and model membranes resembling the pig lens-lipid membrane (**c**, **f**) with different cholesterol contents (see the caption for Fig. 5 for details). Profiles are also included of the oxygen transport parameter across the CBD, which is formed in the POPC membrane, with a cholesterol/POPC mixing ratio of 3/1 (**d**, POPC-CBD), the ESM membrane with a cholesterol/SM mixing ratio of 3 (**e**, SM-CBD) and across model membranes resembling the pig lens-lipid membrane oversaturated with cholesterol at a cholesterol/PL mixing ratio of 2.1/1 (**f**, PL-CBD). *Broken lines* indicate the appropriate value in the aqueous phase. Approximate localizations of nitroxide moieties of spin labels are indicated by *arrows*. Data compiled from Widomska et al. (2007a) and Mainali et al. (2011b)

model membranes with saturating amounts of cholesterol (the CBD was not yet present) and profiles for the same membranes containing coexisting PCDs and CBDs were nearly indistinguishable.

These data suggest that the CBD has some function specific to the fiber-cell plasma membrane. The CBD provides buffering capacity for cholesterol concentration in the surrounding phospholipid bilayer, keeping it at a

constant saturating level and, thus, keeping the physical properties of the membrane consistent and independent of changes in phospholipid composition. Our conclusions are especially significant for human lenses because among mammalian lenses those from humans are of the longest life span and changes in lens phospholipid composition with age are most pronounced (Estrada et al. 2010). Human lens fiber cells undergo minimal cell turnover. They do not regenerate, and cells in the center of the nucleus of an adult human lens are as old as the individual. Membrane proteins that perform several functions in young human lenses perform the same functions in older lenses with altered phospholipid compositions. Thus, the CBD plays a crucial role in maintaining homeostasis of the lens membrane, the only membranous structure of mature fiber cells.

Phospholipid Composition Controls Formation of the CBD

Phospholipids surrounding the CBD cannot affect the properties of its interior because it is a pure cholesterol bilayer (Raguz et al. 2011a, b). However, the phospholipid composition of the fiber-cell plasma membrane can determine the cholesterol concentration at which the CBD is formed. This is a new and uninvestigated mechanism through which cholesterol-dependent processes in the eye lens could be regulated. Our hypothesis is based on the fact that the threshold of cholesterol solubility (expressed here as a Chol/PL molar ratio) differs significantly for simple phospholipid membranes. The values for Chol/PS, Chol/PC, Chol/PE and Chol/SM are 1/2, 1/1, 1/1 and 2/1, respectively (Bach and Wachtel 2003; Epand 2003; Epand et al. 2002; Huang et al. 1999). Here, PS, PC, PE and SM are phosphatidylserine, phosphatidylcholine, phosphatidylethanolamine and ESM, respectively. Above these concentrations, cholesterol forms CBDs in these membranes. PS, PC, PE and SM are major lens phospholipids in humans and other animals (Deeley et al. 2008). Figure 7 presents the hypothetical phase diagram for the mixtures of these lens phospholipids, which shows the cholesterol concentration above which the CBD is formed. It is assumed that the CST value in the phospholipid mixture is a weighted sum of individual thresholds with a weight equal to the mole fraction of the individual phospholipid in the mixture. Thus, the CBD can be formed, depending on the composition of the mixture, already at a cholesterol concentration of 33 mol% (for PS membranes [Raguz et al. 2011a]) up to a cholesterol concentration of 66 mol% (for SM membranes [Mainali et al. 2011d]).

Based on these differences in the CST in different phospholipid bilayers, we can speculate that in animals with a long life span the phospholipid composition of the

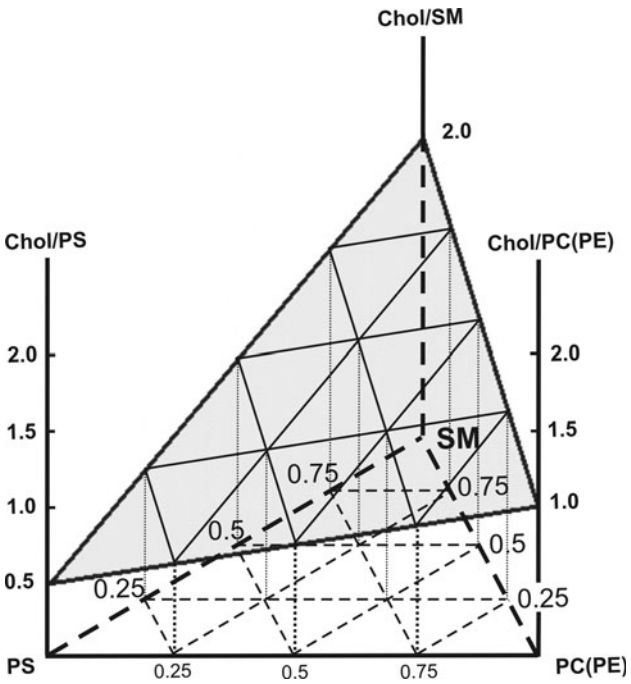

Fig. 7 Hypothetical phase diagram for mixtures of the most abundant lens phospholipids (PS, PC, PE and SM, including dihydrosphingomyelin) and cholesterol. *Shaded surface* indicates the CST for the mixture. For cholesterol contents above this surface, the CBD is formed. It is assumed that the CST value in the phospholipid mixture is a weighted sum of CSTs for individual phospholipids with a weight equal to the mole fraction of the individual phospholipid in the mixture. CSTs in PS, PC, PE and SM membranes are taken from Bach and Wachtel (2003), Epand (2003), Epand et al. (2002) and Huang et al. (1999)

lens membrane (Deeley et al. 2008) ensures formation of CBDs at significantly higher cholesterol concentrations than in animals with a shorter life span. This is illustrated in Fig. 8, where the evaluated value of the CST in the lens-lipid membranes of different animals is plotted as a function of animal life span. It is worth noting that in animals (including humans), the lens phospholipid composition changes with age in a way that delays formation of the CBD. For example, in human lenses the most notable age-related trend is the preferential depletion of glycerophospholipids in older fiber cells and the consequent enrichment of sphingolipids (Yappert and Borchman 2004; Yappert et al. 2003). Thus, the CST in lens-lipid membranes from old donors should be greater than that for young donors. The cholesterol content in lens membranes also increases with age, reaching conditions for CBD formation at a certain age. Thus, the delicate balance between changes in the lens-membrane phospholipid composition and changes in the cholesterol content controls the formation of the CBD. It is also possible that the size of the CBD and the cholesterol exchange rate between the CBD and the PCD are controlled by the lens-membrane phospholipid composition. Most unexpectedly, recent

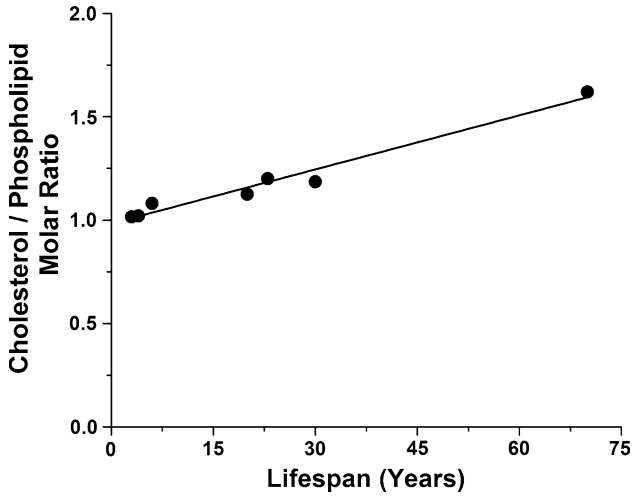

Fig. 8 The relationship between the CST in the lens-lipid membrane and the maximum life spans for different species. CSTs (above these cholesterol contents the CBD should be formed) for lens-lipid membranes were evaluated based on the phospholipid compositions taken from Deeley et al. (2008) and the phase diagram presented in Fig. 7. Points are for mouse (3), rat (4), chick (6), sheep (20), pig (23), cow (30) and human (70) (maximum life-span values are indicated in *parentheses*)

results have shown the high dynamics of cholesterol molecules in the CBD (Raguz et al. 2011a, b), which differ from the rigid organization of cholesterol molecules in cholesterol crystals (Borochov et al. 1995; Cheetham et al. 1989; Epand 2003; Knoll et al. 1985; Mason et al. 2003; Wachtel et al. 1991). This new molecular-level data will help us to better understand the physiological functions of CBDs.

Adult human lenses exhibit extremely high cholesterol contents, with a Chol/PL molar ratio as high as 4, which is much higher than in the lenses of other animals and young humans (Li et al. 1985, 1987; Rujoi et al. 2003; Zelenka 1984). This suggests that in humans, because of an increased amount of sphingolipids, CBDs are formed in aged lenses (first in the lens nucleus, where the cholesterol content is extremely high), while in animals with a shorter life span, the phospholipid composition (high amounts of PS, PC and PE) allows formation of CBDs at much lower cholesterol concentrations (see Deeley et al. 2008 for animal-lens phospholipid compositions).

The CBD Forms a Barrier to Oxygen Transport

Oxygen concentration in the lens is very low, reaching a value close to zero in the lens nucleus (Eaton 1991; Harding 1991; McNulty et al. 2004). Detailed information about oxygen distribution within the lens is scarce: a few measurements have been made that report oxygen partial pressures in the human anterior cortex as low as 0.8–4.0 mmHg (Helbig et al. 1993). At the lens surface, oxygen concentration is low as well (Fig. 1); values of ~ 3 and ~ 9 mmHg have been reported, respectively, at the surface of the anterior and posterior cortex of the lens in the healthy eye (Barbazetto et al. 2004; Bassnett and McNulty 2003; Beebe 2008; Briggs and Rodenhauser 1973; Fitch et al. 2000; Jacobi and Driest 1966; Ormerod et al. 1987; Shui et al. 2006; Siegfried et al. 2010). An increase in oxygen concentration in the lens is thought to be responsible for cataract formation (Borchman et al. 2000; Chung et al. 2001; Freel et al. 2003; Harocopos et al. 2004; Hsuan et al. 2001; Huang et al. 2006, 2008; Palmquist et al. 1984). Thus, understanding the processes that control oxygen transport, concentration and distribution in the lens is very important.

Because oxygen is constantly consumed and oxygen consumption reactions are located inside the eye lens (McNulty et al. 2004), it is concluded that there must be a gradient in the oxygen concentration across fiber-cell layers that builds the eye lens and creates oxygen flux into the lens interior (Fig. 1). Oxygen consumption is necessary to maintain a low oxygen concentration inside the eye lens (otherwise the concentration of oxygen would be equal to that outside the lens). Mitochondrial respiration accounts for approximately 90% of oxygen consumption by the lens (McNulty et al. 2004). This suggests that the outer layers of cortical fiber cells (not yet mature and containing organelles, including mitochondria) could be responsible for a low oxygen concentration in the lens nucleus. Some investigators have proposed that the major function of mitochondria in the lens cortex is not to generate ATP but to maintain lens clarity by keeping the oxygen content very low and preventing proteins and lipids from being oxidized (McNulty et al. 2004). The value of the oxygen concentration difference across certain fiber-cell layers is determined by the rate of oxygen consumption by cells confined inside this concentric fiber-cell layer and the oxygen permeability coefficient of the cell layer. A hypothetical high barrier to oxygen permeation located at the fiber-cell plasma membrane should help to keep oxygen concentration within the eye lens at a very low level. This is especially important for the lens nucleus. A high barrier to oxygen permeation can help to lower oxygen partial pressure in this region to even below that in the cortex if a system to remove oxygen from the nucleus exists. This system should depend on nonmitochondrial oxygen consumption and can be formed by ascorbate- (Eaton 1991; McNulty et al. 2004) or glutathione-dependent oxygen consumption reactions (Beebe et al. 2011). High barriers formed by the membranes of nuclear fiber cells can help to maintain a low oxygen partial pressure in the lens nucleus even at a very low oxygen consumption rate (Fig. 1 helps to illustrate oxygen diffusion into the lens). It should be

stressed that oxygen must pass through thousands of fiber-cell membranes on its way from the lens surface to its center and a very small oxygen concentration difference across each membrane can significantly contribute to the oxygen concentration gradient across the eye lens. Evaluation of how the main lipid domains of fiber-cell membranes contribute to the resistance to oxygen transport into the lens interior is a timely task.

Values of the permeability coefficients for oxygen across the calf (Widomska et al. 2007b), porcine (Raguz et al. 2008), bovine (Raguz et al. 2009) and pig (Mainali personal communication) bulk PCD of the lens-lipid membrane have been reported. At 37°C, they lay in the region from 57.2 to 69.2 cm/s, compared with a value of 69.3 cm/s across a water layer of the same thickness as the membrane. These measurements provide the upper limits for oxygen permeability across the PCD in intact fiber-cell membranes because proteins located in native membranes can decrease oxygen permeability. These problems were discussed by Widomska et al. (2007a).

Oxygen transport across the lens membrane is also affected by CBDs that are formed in the oxygen-permeable lipid bilayer portion of the fiber-cell membrane (Raguz et al. 2008, 2009). However, details of oxygen transport across the CBD are not known and need explanation. As indicated in Fig. 2b, only cholesterol-analogue spin labels, androstane spin label (ASL) and cholestane spin label (CSL), can probe the CBD located within the bulk PCD. Values of the oxygen transport parameter obtained with ASL and CSL for the CBD allowed us to draw an approximate profile of the oxygen transport parameter across this domain (Figs. 4f–h and 6d–f) and calculate its permeability coefficient for oxygen as described in Raguz et al. (2008) and Widomska et al. (2007b). At 37°C, these values lay in the region from 34.4 to 42.5 cm/s, compared with the value of 85.9 cm/s across a water layer of the same thickness as the CBD. The CBD is significantly thinner than the bulk PCD. These data strongly suggest that the major permeability barrier for oxygen transport into the lens interior in the lipid bilayer portion of the fiber-cell plasma membrane is located at the CBD. This should help to maintain a low oxygen concentration in the lens interior and, especially, in the human lens nucleus, where the Chol/PL mole ratio is as high as 4 (Li et al. 1985, 1987) and the CBD should occupy a significant part of the membrane surface. Interestingly, age-related changes in the lipid composition of the human lens (Borchman et al. 1994; Huang et al. 2005; Li et al. 1985, 1987; Rujoi et al. 2003; Truscott 2000) indicate that the resistance of the fiber-cell plasma membrane to oxygen permeation should increase with age and should be greater in the lens nucleus than in the lens cortex (see also discussions in Raguz et al. 2008, 2009; Widomska et al. 2007a, b).

Saturation with Cholesterol Smoothes the Surface of Lens-Lipid Membranes

Another significant structural feature of lens-lipid membranes is the notable steepness of the profiles of the oxygen transport parameter (Fig. 4e–h). These profiles were obtained at 37°C when the lens-lipid membranes (which are saturated with cholesterol) were in the fluid phase. In these membranes, the oxygen transport parameter from the membrane surface to the depth of the ninth carbon is as low as in gel-phase membranes and at locations deeper than the ninth carbon as high as in fluid-phase model membranes without cholesterol. This very sharp (~2.5 times) increase in the oxygen transport parameter occurs within the distance of one carbon–carbon bond (i.e., 1.3–1.5 Å) along the alkyl chain. This transition is smooth and bell-shaped for membranes without cholesterol (Fig. 6d–f) or that contain a small cholesterol concentration (~30 mol%) (Subczynski et al. 1989, 1991, 1998, 2003, 2007b). Abrupt changes that occur in the properties of the fluid-phase membrane are difficult to explain unless it is assumed that at a saturating cholesterol content (1) vertical fluctuations of membrane components are much smaller than in membranes without cholesterol, (2) alignment of all membrane components is high and (3) all cholesterol rings are immersed to the same membrane depth, which is close to the position of C9 in phospholipid alkyl chains. These findings also indicate that by using saturation-recovery EPR and lipid spin labels the main features of the oxygen transport parameter profile can practically be obtained at atomic resolution. Models created through molecular-dynamics simulations (Plesnar et al. 2011) also confirm that saturation with cholesterol narrows the distribution of vertical positions of atoms in phospholipid and cholesterol molecules at any bilayer depth and, as a result, smoothes the membrane surface. Bettelheim and Paunovic (1979) suggested that in a clear human lens most light scattering comes from fiber-cell membranes, whose refractive index is higher than that of the surrounding cytoplasm. Based on this suggestion and data described above, we hypothesize that cholesterol-induced smoothing of the membrane surface should decrease light scattering and help to maintain lens transparency.

Permeability Barriers and Hydrophobic Channels in Membranes Saturated with Cholesterol

The lipid bilayer represents the fundamental permeability barrier to the nonspecific passage of polar molecules into and out of a cell due to its high hydrophobicity. The incorporation of saturating amounts of cholesterol into lens-lipid membranes ensures the rectangular shape of the

hydrophobicity profile across the PCD, with the hydrophobicity in the membrane center comparable to that in hexane and dipropylamine (ε from 2 to 3) (Fig. 4a–d). This greatly increases the activation energy required for polar and small ionic molecules to pass through the membrane. Thus, the rate-limiting step for the permeability of small polar molecules is likely to be the process of crossing the hydrophobic barrier at the membrane center.

The incorporation of saturating amounts of cholesterol also creates resistance to the permeation of small hydrophobic molecules (like oxygen) across the membrane. To better illustrate the transport of oxygen and other small hydrophobic molecules within the lens-lipid membrane saturated and oversaturated with cholesterol, we constructed Fig. 9, in which the inverse of the oxygen transport parameter (which is a measure of resistance to oxygen permeation [Widomska et al. 2007b]) is plotted as a function of the position across the lens-lipid cortical and nuclear membrane of a 2 year old cow. It can be seen that in the PCD of cortical and nuclear membrane, a rather high permeability barrier to oxygen transport is located in the polar headgroup region and, in the hydrophobic region, to the depth of the ninth carbon, which is approximately where the rigid steroid-ring structure of cholesterol reaches into the membrane. Resistance to oxygen permeation in this region is much higher than resistance in the water phase. However, resistance to oxygen permeation in the membrane center is much less than in the water phase and comparable to the resistance in pure phospholipid membranes (see profile for pure POPC bilayer included in Fig. 9). Thus, the rate-limiting step for permeation of small, nonpolar molecules across the membrane (including molecular oxygen) is likely to be the process of crossing the rigidity barrier located near the membrane surface (Raguz et al. 2008, 2009; Widomska et al. 2007b). Similar conclusions can be made for the PCDs of other lens-lipid membranes.

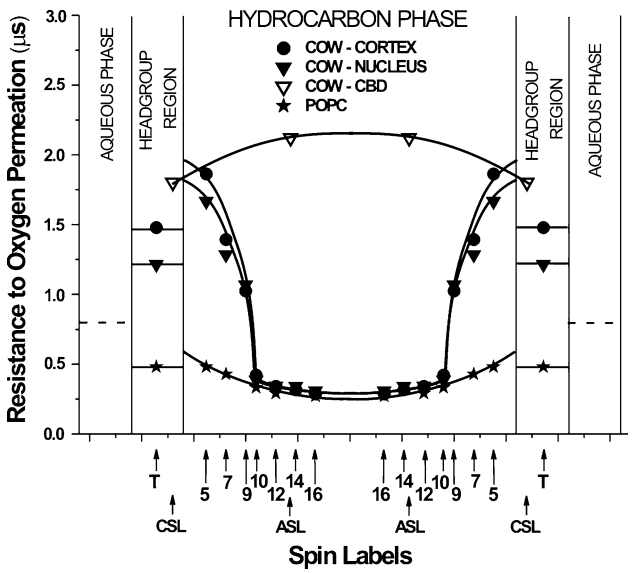

Fig. 9 Profiles of the resistance to oxygen permeation (the inverse of the oxygen transport parameter) across the PCD of lens-lipid membranes made of lipids extracted from the cortex and nucleus of a 2 year old cow at 35°C are plotted to show the oxygen permeability barriers. The profile across the CBD that is formed in lens-lipid membranes made of lipids extracted from a 2 year old cow is also included. To emphasize the effect of cholesterol, the profile of the resistance to oxygen permeation across the pure POPC membrane is shown. The resistance to oxygen permeation in the aqueous phase is indicated as a *broken line*. Oxygen transport parameter values were taken from Fig. 4d, h

These results indicate that the locations of permeation barriers are different for polar and nonpolar molecules. For polar molecules, the major resistance to permeation is the hydrophobic barrier in the central part of the membrane. For nonpolar molecules, the major resistance to permeation is the rigidity barrier near the membrane surface. We can conclude that cholesterol has some functions specific to lens fiber-cell membranes, which are saturated or oversaturated with cholesterol. Since the layers of fiber cells separate the lens interior from the external environment, the membrane barrier must be very high to block nonspecific permeation of small molecules across the membrane into the lens interior. Incorporation of cholesterol into the membrane serves this purpose well because cholesterol simultaneously raises the hydrophobic barrier for polar molecules and increases the rigidity barrier for nonpolar molecules.

Figure 9 also includes the profile of resistance to oxygen permeation across the CBD, coexisting with the PCD, in the nuclear membrane. The resistance to oxygen permeation in this domain is higher than in water and in the surrounding PCD at all depths. In the membrane center, the difference between resistance in the CBD and the PCD is as great as seven times.

Results presented in this review can help us to better understand the molecular nature of the internal barrier to diffusion of small molecules that is formed in the human lens during middle age and is hypothesized to be a key event in the development of age-related nuclear cataract (Moffat et al. 1999; Sweeney and Truscott 1998). The binding of denatured proteins to the fiber-cell membrane as the mechanism responsible for the barrier (Friedrich and Truscott 2009) (possibly by occluding membrane pores and channels) is more probable than a recent hypothesis which states that changes in membrane lipids with age may be responsible (Deeley et al. 2010). The latter mechanism was proposed based on results that revealed that sphingomyelin levels increased with age in the barrier region, until reaching a plateau at approximately 40 years of age. Deeley et al. state that such changes in lipid composition will have a significant impact on the physical properties of

fiber-cell membranes. This contrasts with our conclusion that membrane properties, including barrier properties, are independent of phospholipid composition until the membrane is saturated with cholesterol. However, when the cholesterol concentration is low (~30 mol%), these membranes (especially those composed of saturated sphingomyelin) can be very rigid (Borchman et al. 1996; Kusumi et al. 1986; Wisniewska and Subczynski 2008).

The striking similarity between profiles of the oxygen transport parameter (Figs. 4e–h and 6d–f) and profiles of hydrophobicity (Figs. 4a–d and 6a–c) in lens-lipid membranes and model membranes saturated with cholesterol suggests a possibility for lateral transport of molecular oxygen and other small, nonpolar molecules along the inner core of the membrane (parallel to the membrane surface), which is referred to as "hydrophobic channeling." As shown in Fig. 9, the resistance to the transport of oxygen and other small, hydrophobic molecules in the membrane center is much lower than in the water phase and the solubility of small, hydrophobic molecules is much higher (as indicated by the high hydrophobicity in this region [Figs. 4a–d and 6a–c]). To better illustrate the phenomenon of hydrophobic channeling in lens-lipid membranes, we constructed Fig. 10, in which we display the temperature dependence of the permeability coefficient for oxygen across the membrane region, where the major resistance to oxygen permeation is located (from the membrane surface to the depth of the ninth carbon), and for the membrane center, where oxygen transport is enhanced (between the tenth carbons in each leaflet). To compare the permeability properties of certain membrane regions with those of water, we display these data as a ratio of oxygen permeability across the appropriate membrane region to oxygen permeability across a water layer of the same thickness. We observed that centers of membranes saturated with cholesterol (both lens lipid and model) can serve as channels for oxygen transport as they have a much higher oxygen permeability than water. To escape from these channels, oxygen has to cross high barriers, with low oxygen permeability existing on both sides of the membrane. Additionally, the activation energy for oxygen translational diffusion in the lens-lipid membrane is significantly greater in the region where the rigidity barrier is located than in the membrane center (Raguz et al. 2009). This supports our hypothesis that in the lens-lipid membrane a high cholesterol content is responsible for creating hydrophobic channels for oxygen transport parallel to the membrane surface and, at the same time, a high cholesterol content is responsible for creating the rigidity barrier to oxygen transport across the membrane.

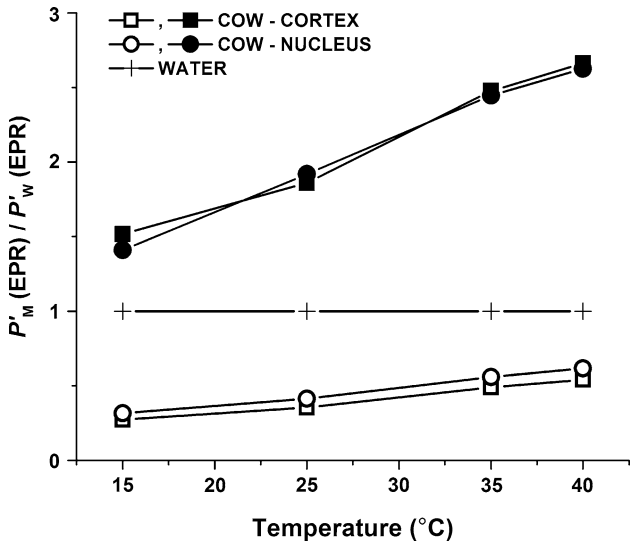

Fig. 10 The permeability coefficient for oxygen across a specific membrane region, P'_M(EPR), relative to that across a water layer of the same thickness as the membrane region, P'_W(EPR)—i.e., P'_M(EPR)/P'_W(EPR)—for cortical and nuclear lens-lipid membranes of a 2 year old cow plotted as a function of temperature. Both P'_M(EPR) and P'_W(EPR) were obtained by the EPR method. *Open symbols* indicate the membrane region from the membrane surface to the depth of the ninth carbon (measurements with T-PC, 5-PC, 7-PC and 9-SASL), and *closed symbols* indicate the membrane region between the tenth carbons in each membrane leaflet (measurements with 10-, 12-, 14- and 16-PC)

Finally, the following question is raised: Is high cholesterol content in the fiber-cell plasma membrane beneficial or harmful to the lens? We addressed this "conflict" of membrane properties in the paper entitled "Membranes: Barriers or Pathways for Oxygen Transport" (Subczynski and Hyde 1998). This conflict is evident in the eye lens, where the barrier to oxygen transport created by fiber-cell plasma membranes can be beneficial, helping to maintain low oxygen partial pressure in the lens nucleus. On the other hand, the hydrophobic channel makes it possible for the system of fiber-cell membranes to form conduits for oxygen molecules from the anterior and posterior surfaces into the deeper regions of the lens. This phenomenon could be harmful to the lens, especially when the low oxygen level around the lens is disturbed. Such an event can occur after vitrectomy, when the partial pressure of oxygen at the posterior of the human lens increases to ~13 mmHg (Siegfried et al. 2010). This increase in oxygen partial pressure is associated with rapid (less than 2 years) opacification of the lens nucleus. Also, in older individuals, when the structure of the vitreous body breaks down (Harocopos et al. 2004), decreasing the rate of ascorbate-dependent oxygen consumption within the vitreous fluid (Shui et al. 2009), the posterior of the lens is exposed to the increased oxygen partial pressure (Beebe et al. 2011). In these conditions, pathways for oxygen transport provided by the fiber-cell membranous system supply more oxygen to the lens center, disturbing the delicate balance between oxygen consumption and oxygen delivery and increasing

oxygen partial pressure in the lens nucleus, which, as a consequence, leads to cataract development.

Concluding Remarks

In our opinion, the amount of data collected for lens-lipid membranes and model membranes saturated and oversaturated with cholesterol is sufficient to determine the significant functions of cholesterol and CBDs specific to the fiber-cell plasma membranes of the eye lens. Mechanisms of these functions, which manifest themselves through cholesterol-induced changes in the properties and organization of the lipid bilayer portion of the fiber-cell plasma membrane, are explained on the molecular level. This was possible thanks to the abilities of molecular probe methods (EPR spin labeling) using phospholipid- and cholesterol-analogue spin labels. The local information coming from the small nitroxide moiety (attached to a specific position of the lipid molecules) allowed us to build a fairly complete three-dimensional dynamic structure of the lens lipid membrane and to obtain three-dimensional distribution of membrane properties. In this case, "three-dimensional" means the ability to get information about the lateral organization of the membrane (including coexisting domains) and to obtain membrane properties in each domain as a function of the third dimension (namely, the membrane depth).

We are aware of the limitations of the conclusions and hypotheses presented in this review, which were made based on measurements using lens-lipid membranes formed from lipids extracted from eye lenses. Intact eye-lens membranes are loaded with membrane proteins, which raises questions and concerns as to what extent the conclusions presented above can apply. These concerns outline the future direction of our work, which requires that experiments are performed with intact membranes and, possibly, with simple reconstituted membranes made of lens-lipid extracts and lens-membrane proteins.

Our study of the functions of cholesterol in simple models should also help us to better understand its functions in intact membranes. Such steps in the investigation of the properties and organization of the lipid-bilayer portion of fiber-cell plasma membranes are necessary. Without this research, it is not possible to understand clearly the mechanisms by which intrinsic proteins affect the properties of the lipid bilayer. We will investigate the properties of the lipid-bilayer portion of intact lens membranes further; but it is not an easy task, and it will take some time to clarify existing methodological problems before results can be obtained with the same confidence we have in our lens-lipid membrane measurements. However, based on data from the literature and our own studies, we can predict major changes in the properties of the lipid-bilayer portion of intact fiber-cell plasma membranes (which are dense with integral membrane proteins) compared to the properties of lens-lipid membranes. Lipids around monomers of integral membrane proteins are more immobilized than bulk lipids (Jost et al. 1973; Ryba et al. 1987), and even more immobilized are lipids trapped within aggregates of integral membrane proteins (Ashikawa et al. 1994). Additionally, oxygen permeability across boundary and bulk lipid domains is strongly reduced (Ashikawa et al. 1994; Kawasaki et al. 2001). Because proteins are nearly impermeable to oxygen (Altenbach et al. 1994; Subczynski et al. 1992), the effective oxygen permeability coefficient across the fiber-cell plasma membrane should be equal to the oxygen permeability coefficient evaluated for the lipid-bilayer portion of the membrane multiplied by a factor proportional to the surface area of the lipid-bilayer portion and divided by the surface area of the entire membrane. Thus, we can conclude that the intact fiber-cell membrane forms a significantly greater barrier to oxygen permeation than the lens-lipid membrane.

At this stage, the conclusions presented here are valid for model membranes, and our investigations have filled a gap in membrane research by providing profiles of physical properties across membranes saturated and oversaturated with cholesterol. Profiles are also valid for membranes that contain a small amount of membrane proteins, where the amount of bulk lipids exceeds the amount of lipids in immediate contact with proteins.

Acknowledgements This work was supported by grants EY015526, TW008052, EB002052 and EB001980 of the National Institutes of Health.

References

Altenbach C, Greenhalgh DA, Khorana HG, Hubbell WL (1994) A collision gradient method to determine the immersion depth of nitroxides in lipid bilayers: application to spin-labeled mutants of bacteriorhodopsin. Proc Natl Acad Sci USA 91:1667–1671

Ashikawa I, Yin J-J, Subczynski WK, Kouyama T, Hyde JS, Kusumi A (1994) Molecular organization and dynamics in bacteriorhodopsin-rich reconstituted membranes: discrimination of lipid environments by the oxygen transport parameter using a pulse ESR spin-labeling technique. Biochemistry 33:4947–4952

Bach D, Wachtel E (2003) Phospholipid/cholesterol model membranes: formation of cholesterol crystallites. Biochim Biophys Acta 1610:187–197

Barbazetto IA, Liang J, Chang S, Zheng L, Spector A, Dillon JP (2004) Oxygen tension in the rabbit lens and vitreous before and after vitrectomy. Exp Eye Res 78:917–924

Bassnett S, McNulty R (2003) The effect of elevated intraocular oxygen on organelle degradation in the embryonic chicken lens. J Exp Biol 206:4353–4361

Beebe DC (2003) The lens. In: Kaufman PL (ed) Physiology of the eye. Mosby-Year Book, St. Louis, pp 117–158

Beebe DC (2008) Maintaining transparency: a review of the developmental physiology and pathophysiology of two avascular tissues. Semin Cell Dev Biol 19:125–133

Beebe DC, Holekamp NM, Siegfried C, Shui YB (2011) Vitreoretinal influences on lens function and cataract. Phil Trans R Soc Lond B Biol Sci 366:1293–1300

Bettelheim FA, Paunovic M (1979) Light scattering of normal human lens I. Application of random density and orientation fluctuation theory. Biophys J 26:85–99

Biswas SK, Lo WK (2007) Gap junctions contain different amounts of cholesterol which undergo unique sequestering processes during fiber cell differentiation in the embryonic chicken lens. Mol Vis 13:345–359

Biswas SK, Jiang JX, Lo WK (2009) Gap junction remodeling associated with cholesterol redistribution during fiber cell maturation in the adult chicken lens. Mol Vis 15:1492–1508

Biswas SK, Lee JE, Brako L, Jiang JX, Lo WK (2010) Gap junctions are selectively associated with interlocking ball-and-sockets but not protrusions in the lens. Mol Vis 16:2328–2341

Borchman D, Yappert MC (2010) Lipids and the ocular lens. J Lipid Res 51:2473–2488

Borchman D, Delamere NA, Cauley LA, Paterson CA (1989) Studies on the distribution of cholesterol, phospholipid and protein in the human and bovine lens. Lens Eye Exp Res 6:703–724

Borchman D, Lamba OP, Yappert MC (1993) Structural characterization of lipid membranes from clear and cataractous human lenses. Exp Eye Res 57:199–208

Borchman D, Byrdwell WC, Yappert MC (1994) Regional and age-dependent differences in the phospholipid composition of human lens membranes. Invest Ophthalmol Vis Sci 35:3938–3942

Borchman D, Cenedella RJ, Lamba OP (1996) Role of cholesterol in the structural order of lens membrane lipids. Exp Eye Res 62:191–197

Borchman D, Tang D, Yappert MC (1999) Lipid composition, membrane structure relationships in lens and muscle sarcoplasmic reticulum membranes. Biospectroscopy 5:151–167

Borchman D, Giblin FJ, Leverenz VR, Reddy VN, Lin LR, Yappert MC, Tang D, Li L (2000) Impact of aging and hyperbaric oxygen in vivo on guinea pig lens lipids and nuclear light scatter. Invest Ophthalmol Vis Sci 41:3061–3073

Borchman D, Yappert MC, Afzal M (2004) Lens lipids and maximum lifespan. Exp Eye Res 79:761–768

Borochov N, Wachtel EJ, Bach D (1995) Phase behavior of mixtures of cholesterol and saturated phosphatidylglycerols. Chem Phys Lipids 76:85–92

Briggs D, Rodenhauser JH (1973) Distribution and consumption of oxygen in the vitreous body of cats. In: Kessler M (ed) Oxygen supply: theoretical and practical aspects of oxygen supply and microcirculation of tissue. University Park Press, Baltimore, pp 265–269

Broekhuyse RM (1973) Membrane lipids and proteins in aging lens and cataract. Ciba Found Symp 19:135–149

Broekhuyse RM, Kuhlmann ED (1974) Lens membranes 1. Composition of urea-treated plasma membranes from calf lens. Exp Eye Res 19:297–302

Broekhuyse RM, Kuhlmann ED (1978) Lens membranes. IV. Preparative isolation and characterization of membranes and various membrane proteins from calf lens. Exp Eye Res 26:305–320

Cenedella RJ (1996) Cholesterol and cataracts. Surv Ophthalmol 40:320–337

Cheetham JJ, Wachtel E, Bach D, Epand RM (1989) Role of the stereochemistry of the hydroxyl group of cholesterol and the formation of nonbilayer structures in phosphatidylethanolamines. Biochemistry 28:8928–8934

Chung CP, Hsu SY, Wu WC (2001) Cataract formation after pars plana vitrectomy. Kaohsiung J Med Sci 17:84–89

de Vries AC, Cohen LH (1993) Different effects of the hypolipidemic drugs pravastatin and lovastatin on the cholesterol biosynthesis of the human ocular lens in organ culture and on the cholesterol content of the rat lens in vivo. Biochim Biophys Acta 1167: 63–69

Deeley JM, Mitchell TW, Wei X, Korth J, Nealon JR, Blanksby SJ, Truscott RJ (2008) Human lens lipids differ markedly from those of commonly used experimental animals. Biochim Biophys Acta 1781:288–298

Deeley JM, Hankin JA, Friedrich MG, Murphy RC, Truscott RJ, Mitchell TW, Blanksby SJ (2010) Sphingolipid distribution changes with age in the human lens. J Lipid Res 51:2753–2760

Eaton JW (1991) Is the lens canned? Free Radic Biol Med 11: 207–213

Epand RM (2003) Cholesterol in bilayers of sphingomyelin or dihydrosphingomyelin at concentrations found in ocular lens membranes. Biophys J 84:3102–3110

Epand RM (2005) Role of membrane lipids in modulating the activity of membrane-bound enzymes. In: Yeagle PL (ed) The structure of biological membrane. CRC Press, Boca Raton, pp 499–509

Epand RM, Bain AD, Sayer BG, Bach D, Wachtel E (2002) Properties of mixtures of cholesterol with phosphatidylcholine or with phosphatidylserine studied by ^{13}C magic angle spinning nuclear magnetic resonance. Biophys J 83:2053–2063

Estrada R, Puppato A, Borchman D, Yappert MC (2010) Reevaluation of the phospholipid composition in membranes of adult human lenses by ^{31}P NMR and MALDI MS. Biochim Biophys Acta 1798:303–311

Fitch CL, Swedberg SH, Livesey JC (2000) Measurement and manipulation of the partial pressure of oxygen in the rat anterior chamber. Curr Eye Res 20:121–126

Fleschner CR, Cenedella RJ (1991) Lipid composition of lens plasma membrane fractions enriched in fiber junctions. J Lipid Res 32: 45–53

Freel CD, Gilliland KO, Mekeel HE, Giblin FJ, Costello MJ (2003) Ultrastructural characterization and Fourier analysis of fiber cell cytoplasm in the hyperbaric oxygen treated guinea pig lens opacification model. Exp Eye Res 76:405–415

Friedrich MG, Truscott RJ (2009) Membrane association of proteins in the aging human lens: profound changes take place in the fifth decade of life. Invest Ophthalmol Vis Sci 50:4786–4793

Harding JJ (1991) Cataract, biochemistry, epidemiology and pharmacology. Chapman and Hall, London

Harocopos GJ, Shui YB, McKinnon M, Holekamp NM, Gordon MO, Beebe DC (2004) Importance of vitreous liquefaction in age-related cataract. Invest Ophthalmol Vis Sci 45:77–85

Helbig H, Hinz JP, Kellner U, Foerster MH (1993) Oxygen in the anterior chamber of the human eye. Ger J Ophthalmol 2:161–164

Hsuan JD, Brown NA, Bron AJ, Patel CK, Rosen PH (2001) Posterior subcapsular and nuclear cataract after vitrectomy. J Cataract Refract Surg 27:437–444

Huang J, Buboltz JT, Feigenson GW (1999) Maximum solubility of cholesterol in phosphatidylcholine and phosphatidylethanolamine bilayers. Biochim Biophys Acta 1417:89–100

Huang L, Grami V, Marrero Y, Tang D, Yappert MC, Rasi V, Borchman D (2005) Human lens phospholipid changes with age and cataract. Invest Ophthalmol Vis Sci 46:1682–1689

Huang L, Estrada R, Yappert MC, Borchman D (2006) Oxidation-induced changes in human lens epithelial cells. 1. Phospholipids. Free Radic Biol Med 41:1425–1432

Huang L, Yappert MC, Jumblatt MM, Borchman D (2008) Hyperoxia and thyroxine treatment and the relationships between reactive oxygen species generation, mitochondrial membrane potential, and cardiolipin in human lens epithelial cell cultures. Curr Eye Res 33:575–586

Hubbell WL, McConnell HM (1968) Spin-label studies of the excitable membranes of nerve and muscle. Proc Natl Acad Sci USA 61:12–16

Jacob RF, Cenedella RJ, Mason RP (1999) Direct evidence for immiscible cholesterol domains in human ocular lens fiber cell plasma membranes. J Biol Chem 274:31613–31618

Jacob RF, Cenedella RJ, Mason RP (2001) Evidence for distinct cholesterol domains in fiber cell membranes from cataractous human lenses. J Biol Chem 276:13573–13578

Jacobi KW, Driest J (1966) Oxygen determinations in the vitreous body of the living eye [in German]. Ber Zusammenkunft Dtsch Ophthalmol Ges 67:193–198

Jost PC, Griffith OH, Capaldi RA, Vanderkooi G (1973) Evidence for boundary lipid in membranes. Proc Natl Acad Sci USA 70:480–484

Kawasaki K, Yin J–J, Subczynski WK, Hyde JS, Kusumi A (2001) Pulse EPR detection of lipid exchange between protein rich raft and bulk domains in the membrane: methodology development and its application to studies of influenza viral membrane. Biophys J 80:738–748

Kirby TJ (1967) Cataracts produced by triparanol (MER-29). Trans Am Ophthalmol Soc 65:494–543

Knoll W, Schmidt G, Ibel K, Sackmann E (1985) Small-angle neutron scattering study of lateral phase separation in dimyristoylphosphatidylcholine-cholesterol mixed membranes. Biochemistry 24:5240–5246

Kusumi A, Subczynski WK, Hyde JS (1982) Oxygen transport parameter in membranes as deduced by saturation recovery measurements of spin-lattice relaxation times of spin labels. Proc Natl Acad Sci USA 79:1854–1858

Kusumi A, Subczynski WK, Pasenkiewicz-Gierula M, Hyde JS, Merkle H (1986) Spin-label studies on phosphatidylcholine-cholesterol membranes: effects of alkyl chain length and unsaturation in the fluid phase. Biochim Biophys Acta 854:307–317

Li LK, So L (1987) Age dependent lipid and protein changes in individual bovine lenses. Curr Eye Res 6:599–605

Li LK, So L, Spector A (1985) Membrane cholesterol and phospholipid in consecutive concentric sections of human lenses. J Lipid Res 26:600–609

Li LK, So L, Spector A (1987) Age-dependent changes in the distribution and concentration of human lens cholesterol and phospholipids. Biochim Biophys Acta 917:112–120

Mainali L, Feix JB, Hyde JS, Subczynski WK (2011a) Membrane fluidity profiles as deduced by saturation-recovery EPR measurements of spin-lattice relaxation times of spin labels. J Magn Reson 212:418–425

Mainali L, Raguz M, Camenisch TG, Hyde JS, Subczynski WK (2011b) Spin-label saturation-recovery EPR at W-band: applications to eye lens lipid membranes. J Magn Reson 212:86–94

Mainali L, Raguz M, Subczynski WK (2011c). Phases and domains in sphingomyelin-cholesterol membranes: structure and properties using EPR spin-labeling methods. Eur Biophys J. doi:10.1007/s00249-011-0766-4

Mainali L, Raguz M, Subczynski WK (2011d) Phase-separation and domain-formation in cholesterol-sphingomyelin mixture: pulse-EPR oxygen probing. Biophys J 101:837–846

Marsh D (1981) Electron spin resonance: spin labels. In: Grell E (ed) Membrane spectroscopy. Springer-Verlag, Berlin, pp 51–142

Mason RP, Tulenko TN, Jacob RF (2003) Direct evidence for cholesterol crystalline domains in biological membranes: role in human pathobiology. Biochim Biophys Acta 1610:198–207

McNulty R, Wang H, Mathias RT, Ortwerth BJ, Truscott RJ, Bassnett S (2004) Regulation of tissue oxygen levels in the mammalian lens. J Physiol 559:883–898

Moffat BA, Landman KA, Truscott RJ, Sweeney MH, Pope JM (1999) Age-related changes in the kinetics of water transport in normal human lenses. Exp Eye Res 69:663–669

Mosley ST, Kalinowski SS, Schafer BL, Tanaka RD (1989) Tissue-selective acute effects of inhibitors of 3-hydroxy-3-methylglutaryl coenzyme A reductase on cholesterol biosynthesis in lens. J Lipid Res 30:1411–1420

Ormerod LD, Edelstein MA, Schmidt GJ, Juarez RS, Finegold SM, Smith RE (1987) The intraocular environment and experimental anaerobic bacterial endophthalmitis. Arch Ophthalmol 105: 1571–1575

Palmquist BM, Philipson B, Barr PO (1984) Nuclear cataract and myopia during hyperbaric oxygen therapy. Br J Ophthalmol 68:113–117

Plesnar E, Subczynski WK, Pasenkiewicz-Gierula, M (2011). Saturation with cholesterol increases vertical order and smoothes the surface of the phosphatidylcholine bilayer: a molecular simulation study. Biochim Biophys Acta. doi:10.1016/j.bbamem.2011.10.023

Paterson CA, Zeng J, Husseini Z, Borchman D, Delamere NA, Garland D, Jimenez-Asensio J (1997) Calcium ATPase activity and membrane structure in clear and cataractous human lenses. Curr Eye Res 16:333–338

Peterson CA, Delamere NA (1992) The lens. In: Hart WM Jr (ed) Physiology of the eye. Mosby-Year Book, St. Louis, pp 348–390

Rafferty NS (1985) Lens morphology. In: Maisel H (ed) The ocular lens: structure, function and pathology. Marcel Dekker, New York, pp 1–60

Raguz M, Widomska J, Dillon J, Gaillard ER, Subczynski WK (2008) Characterization of lipid domains in reconstituted porcine lens membranes using EPR spin-labeling approaches. Biochim Biophys Acta 1778:1079–1090

Raguz M, Widomska J, Dillon J, Gaillard ER, Subczynski WK (2009) Physical properties of the lipid bilayer membrane made of cortical and nuclear bovine lens lipids: EPR spin-labeling studies. Biochim Biophys Acta 1788:2380–2388

Raguz M, Mainali L, Widomska J, Subczynski WK (2011a) The immiscible cholesterol bilayer domain exists as an integral part of phospholipid bilayer membranes. Biochim Biophys Acta 1808:1072–1080

Raguz M, Mainali L, Widomska J, Subczynski WK (2011b). Using spin-label electron paramagnetic resonance (EPR) to discriminate and characterize the cholesterol bilayer domain. Chem Phys Lipids 164:819–829

Rouser G, Solomon RD (1969) Changes in phospholipid composition of human aorta with age. Lipids 4:232–234

Rouser G, Simon G, Kritchevsky G (1969) Species variations in phospholipid class distribution of organs. I. Kidney, liver and spleen. Lipids 4:599–606

Rouser G, Yamamoto A, Kritchevsky G (1971) Cellular membranes. Structure and regulation of lipid class composition species differences, changes with age, and variations in some pathological states. Arch Intern Med 127:1105–1121

Roy D, Rosenfeld L, Spector A (1982) Lens plasma membrane: isolation and biochemical characterization. Exp Eye Res 35: 113–129

Rujoi M, Jin J, Borchman D, Tang D, Yappert MC (2003) Isolation and lipid characterization of cholesterol-enriched fractions in cortical and nuclear human lens fibers. Invest Ophthalmol Vis Sci 44:1634–1642

Rujoi M, Estrada R, Yappert MC (2004) In situ MALDI-TOF MS regional analysis of neutral phospholipids in lens tissue. Anal Chem 76:1657–1663

Ryba NJ, Horvath LI, Watts A, Marsh D (1987) Molecular exchange at the lipid–rhodopsin interface: spin-label electron spin resonance studies of rhodopsin-dimyristoylphosphatidylcholine recombinants. Biochemistry 26:3234–3240

Shui YB, Fu JJ, Garcia C, Dattilo LK, Rajagopal R, McMillan S, Mak G, Holekamp NM, Lewis A, Beebe DC (2006) Oxygen distribution in the rabbit eye and oxygen consumption by the lens. Invest Ophthalmol Vis Sci 47:1571–1580

Shui YB, Holekamp NM, Kramer BC, Crowley JR, Wilkins MA, Chu F, Malone PE, Mangers SJ, Hou JH, Siegfried CJ, Beebe DC (2009) The gel state of the vitreous and ascorbate-dependent oxygen consumption: relationship to the etiology of nuclear cataracts. Arch Ophthalmol 127:475–482

Siegfried CJ, Shui YB, Holekamp NM, Bai F, Beebe DC (2010) Oxygen distribution in the human eye: relevance to the etiology of open-angle glaucoma after vitrectomy. Invest Ophthalmol Vis Sci 51:5731–5738

Subczynski WK, Hyde JS (1998) Membranes. Barriers or pathways for oxygen transport. Adv Exp Med Biol 454:399–408

Subczynski WK, Hyde JS, Kusumi A (1989) Oxygen permeability of phosphatidylcholine-cholesterol membranes. Proc Natl Acad Sci USA 86:4474–4478

Subczynski WK, Hyde JS, Kusumi A (1991) Effect of alkyl chain unsaturation and cholesterol intercalation on oxygen transport in membranes: a pulse ESR spin labeling study. Biochemistry 30:8578–8590

Subczynski WK, Renk GE, Crouch RK, Hyde JS, Kusumi A (1992) Oxygen diffusion-concentration product in rhodopsin as observed by a pulse ESR spin labeling method. Biophys J 63: 573–577

Subczynski WK, Wisniewska A, Yin J-J, Hyde JS, Kusumi A (1994) Hydrophobic barriers of lipid bilayer membranes formed by reduction of water penetration by alkyl chain unsaturation and cholesterol. Biochemistry 33:7670–7681

Subczynski WK, Lewis RN, McElhaney RN, Hodges RS, Hyde JS, Kusumi A (1998) Molecular organization and dynamics of 1-palmitoyl-2-oleoylphosphatidylcholine bilayers containing a transmembrane alpha-helical peptide. Biochemistry 37:3156–3164

Subczynski WK, Pasenkiewicz-Gierula M, McElhaney RN, Hyde JS, Kusumi A (2003) Molecular dynamics of 1-palmitoyl-2-oleoylphosphatidylcholine membranes containing transmembrane alpha-helical peptides with alternating leucine and alanine residues. Biochemistry 42:3939–3948

Subczynski WK, Widomska J, Wisniewska A, Kusumi A (2007a) Saturation-recovery electron paramagnetic resonance discrimination by oxygen transport (DOT) method for characterizing membrane domains. Methods Mol Biol 398:143–157

Subczynski WK, Wisniewska A, Hyde JS, Kusumi A (2007b) Three-dimensional dynamic structure of the liquid-ordered domain as examined by a pulse-EPR oxygen probing. Biophys J 92:1573–1584

Subczynski WK, Raguz M, Widomska J (2010) Studying lipid organization in biological membranes using liposomes and EPR spin labeling. Methods Mol Biol 606:247–269

Sweeney MH, Truscott RJ (1998) An impediment to glutathione diffusion in older normal human lenses: a possible precondition for nuclear cataract. Exp Eye Res 67:587–595

Truscott RJ (2000) Age-related nuclear cataract: a lens transport problem. Ophthalmic Res 32:185–194

Tulenko TN, Chen M, Mason PE, Mason RP (1998) Physical effects of cholesterol on arterial smooth muscle membranes: evidence of immiscible cholesterol domains and alterations in bilayer width during atherogenesis. J Lipid Res 39:947–956

Wachtel EJ, Borochov N, Bach D (1991) The effect of protons or calcium ions on the phase behavior of phosphatidylserine-cholesterol mixtures. Biochim Biophys Acta 1066:63–69

Widomska J, Raguz M, Dillon J, Gaillard ER, Subczynski WK (2007a) Physical properties of the lipid bilayer membrane made of calf lens lipids: EPR spin labeling studies. Biochim Biophys Acta 1768:1454–1465

Widomska J, Raguz M, Subczynski WK (2007b) Oxygen permeability of the lipid bilayer membrane made of calf lens lipids. Biochim Biophys Acta 1768:2635–2645

Wisniewska A, Subczynski WK (2008) The liquid-ordered phase in sphingomyelin-cholesterol membranes as detected by the discrimination by oxygen transport (DOT) method. Cell Mol Biol Lett. 13:430–451

Yappert MC, Borchman D (2004) Sphingolipids in human lens membranes: an update on their composition and possible biological implications. Chem Phys Lipids 129:1–20

Yappert MC, Rujoi M, Borchman D, Vorobyov I, Estrada R (2003) Glycero- versus sphingo-phospholipids: correlations with human and non-human mammalian lens growth. Exp Eye Res 76:725–734

Zelenka PS (1984) Lens lipids. Curr Eye Res 3:1337–1359